

Identification of Glycolaldehyde Enol (HOHC=CHOH) in Interstellar Analogue Ices

N. Fabian Kleimeier,* André K. Eckhardt,* and Ralf I. Kaiser*



Cite This: *J. Am. Chem. Soc.* 2021, 143, 14009–14018



Read Online

ACCESS |



Metrics & More

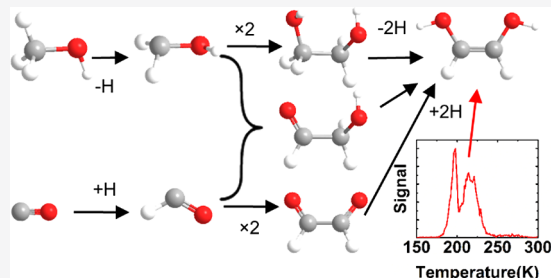


Article Recommendations



Supporting Information

ABSTRACT: Glycolaldehyde is considered the entry point in the aqueous prebiotic formose (Butlerow) reaction although it mainly exists in its unreactive hydrated form in aqueous solution. The characterization of the more reactive nucleophilic enol form under interstellar conditions has remained elusive to date. Here we report on the identification of glycolaldehyde enol (1,2-ethenediol, HOHC=CHOH) in low temperature methanol-bearing ices at temperatures as low as 5 K. Exploiting isotope labeling and isomer-selective photoionization coupled with reflectron time-of-flight mass spectrometry, our results unravel distinct reaction pathways to 1,2-ethenediol, thus demonstrating the kinetic stability, availability for prebiotic sugar formation, and potential detectability in deep space.



INTRODUCTION

The formation of carbohydrates in prebiotic chemistry is often connected to the *formose* or Butlerow reaction.^{1–4} Hereby various aldoses and ketoses form unselectively in basic aqueous formaldehyde (H₂CO, 1) solutions at elevated temperatures. In an initial step glycolaldehyde (HOCH₂CHO, 2) slowly forms which according to Breslow further serves as a kind of autocatalyst for the production of higher carbohydrates by base-catalyzed aldol carbon–carbon bond-forming reactions.^{2,3} However, in aqueous solution glycolaldehyde mainly exists in its unreactive hydrated form.⁵ Basic conditions enable keto–enol tautomerism to produce glycolaldehyde enol (*E/Z*-1,2-ethenediol, HOHC=CHOH, 3), the reactive form of 2 and key intermediate in further sugar-forming reactions.³ The enol serves as a nucleophile in the reaction with electrophilic carbonyl compounds via a favorable six-membered six-electron transition state to form glyceraldehyde (4) in a first step (Figure 1a). Isomerization of glyceraldehyde to the thermodynamically preferred dihydroxyacetone (HOCH₂C(O)CH₂OH) occurs via [1,2]hydride shift reactions^{3,4} and enables branched ketose synthesis in formose type reactions and, for example, the prebiotic synthesis of DNA nucleosides.⁶ Borate minerals were shown to stabilize ribose, the backbone of RNA, in complex formose mixtures.⁷ Alternative prebiotic scenarios for sugar synthesis have been demonstrated including, for example, HCN photoredox photochemistry in aqueous solution,⁸ mechanochemically induced formose reaction in the absence of water,⁹ or a barrierless carbonyl ene type reaction of hydroxymethylene (H–C̈–OH) and carbonyl compounds under interstellar conditions.^{10,11}

However, efficient sugar formation in the classical formose reaction typically requires elevated temperatures, basic aqueous conditions, and the availability of calcium ions to stabilize the

reactive 1,2-ethenediol intermediate, limiting the scenarios under which sugars could form on, for example, prehistoric Earth or meteors that ultimately deliver those sugars to other planets. Laboratory studies exposing interstellar model ices to ionizing radiation have demonstrated that the abiotic formation of biologically relevant molecules is feasible under interstellar conditions. This implies that key biological compounds such as sugars and amino acids might form on ice-coated interstellar grains, the raw material for solar systems, by energetic processing in cold molecular clouds at temperatures as low as 10 K. Those organics are eventually incorporated into parent bodies of meteorites and can further be energetically processed in their icy mantle on their journey through space. Parts of these organic molecules can survive entry into the atmosphere of other planets like Earth.¹² In fact, many molecules that were detected in energetically processed interstellar model ices in laboratory experiments were also found in meteorite samples: glycerol (CH₂OHCH(OH)CH₂OH) was formed in the laboratory in methanol model ices¹³ and found in the Murchison meteorite,^{14,15} and pyruvic acid (CH₃COCOOH) was detected in binary ices of acetaldehyde and carbon dioxide¹⁶ and detected in Alan Hill.¹⁷ Furthermore, carbohydrates, including glyceraldehyde, dihydroxyacetone, and ribose, were detected after ultraviolet (UV) irradiation of ternary mixtures of water, methanol, and ammonia (NH₃)^{18,19} and have also been found

Received: August 1, 2021

Published: August 19, 2021



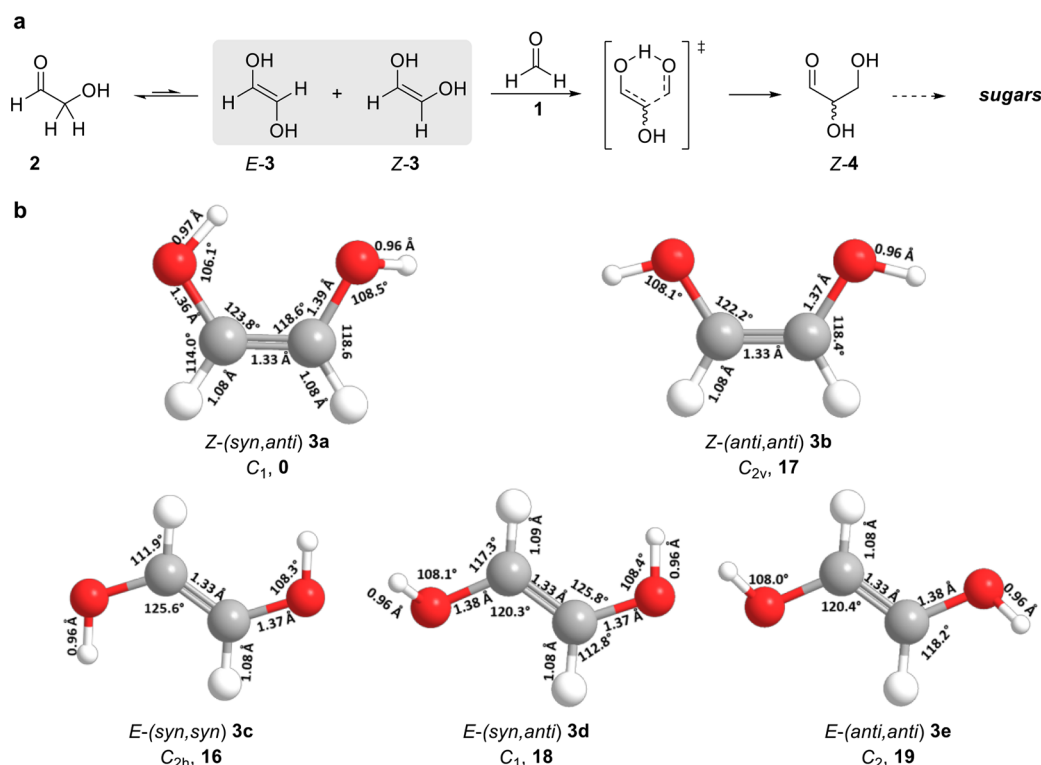


Figure 1. Aldol reaction with chemically feasible six-membered transition states enable new carbon–carbon bond formation and sugar-producing chemistry (a). Five conformers of 1,2-ethenediol (3) with point groups and relative energies in kJ mol^{-1} (bold) at the AE-CCSD(T)/cc-pWCVTZ level + zero-point vibrational energy (b).

in the Murchison meteorite.^{14,15} Lastly, amino acids were detected in the Murchison meteorite²⁰ and in the coma of 67P/Churyumov–Gerasimenko²¹ and were also formed in interstellar model ices after irradiation.²²

However, fundamental reaction mechanisms leading to biorelevant organics are still lacking. An identification of reactive intermediates such as enols is of particular importance to our understanding how sugars might form via molecular mass growth processes from the bottom up.² However, considering the lack of suitable precursors and difficulty in preparation, simple enols represent one of the least explored classes of biorelevant organic molecules to date.^{23–25} Consequently, gas-phase aldol reactions have also not been studied experimentally. 1,2-Ethenediol has, up to now, only been tentatively inferred as a possible byproduct in the fragmentation of the transition metal complex $[\text{HOCD}_2\text{CD}_2\text{OH}\cdots\text{Zn}^{2+}\cdots\text{OOCCH}_3]$ ²⁶ and in an infrared and NMR study of the flash pyrolysis products of dihydroxy-11,12-ethano-9,10-dihydro-9,10-anthracene.²⁷

Here, we demonstrate the *formation* and *isomer-selective mass spectrometric identification* of 3 in interstellar model ices consisting of methanol (CH_3OH , 5) and methanol–carbon monoxide (CO, 6), respectively, processed with energetic electrons mimicking galactic cosmic ray (GCR) exposure of ice-coated interstellar grains over typical lifetimes of molecular clouds of a few 10^6 years.^{28,29} These ice mixtures were chosen because previous studies demonstrated the facile formation of 2 in these ices.³⁰ Interstellar ices containing carbon monoxide and methanol at levels of up to 50% and 30%, respectively, were observed toward high- and low-mass star-forming regions.^{31,32}

Theoretically five conformers of 3 exist, with the C_{1v} symmetric Z-(syn,anti)-configuration (3a) as the thermodynamically preferred species according to our CCSD(T)/cc-pWCVTZ + zero-point vibrational energy (ZPVE) computations (Figure 1b,

Table S1). The remaining conformers are 16–19 kJ mol^{-1} higher in energy considering the absence of intramolecular hydrogen bonding. The detection of the keto–enol pair acetaldehyde–vinyl alcohol in the star-forming region SgrB2 demonstrates that enols are kinetically stable in the interstellar medium, and unimolecular isomerization to their thermodynamically preferred keto form does not occur.³³ Considering that glycolaldehyde has also been detected toward SgrB2,^{34,35} our results propose that conformers of 3 might also be present there and should be searched for in the gas phase through their rotational spectra thus shining light on the fundamental processes advancing the organic chemistry in these extreme environments.

EXPERIMENTAL DETAILS

Experiments were conducted in a stainless steel ultrahigh vacuum chamber pumped to 5×10^{-11} Torr by magnetically levitated turbomolecular pumps backed by a hydrocarbon-free scroll pump. A polished silver substrate was interfaced to a rotatable cold head that was cooled to 5 K by a closed-cycle helium compressor (Sumitomo Heavy Industries, RDK-415E). Methanol was filled into a glass vial interfaced to a UHV chamber, and residual atmospheric gases were removed by subjecting it to several freeze–thaw cycles at liquid nitrogen temperatures. Gases used in the experiment were supplied to the main UHV chamber through separate glass capillary arrays to a total background pressure of 5×10^{-8} Torr. The thickness of the ices was determined during deposition by recording interference patterns of a helium–neon laser. After deposition, infrared spectra of the pristine ices were recorded using a Nicolet 6700 FTIR spectrometer (Fisher Scientific) before subjecting them to 5 keV electrons at a current of 30 nA for 60 min while continuously recording IR spectra to monitor radiation-induced changes. Monte Carlo simulations were performed using the CASINO software suite³⁶ to calculate the dose and to ensure that the ice was thick enough so that no electrons were transmitted to

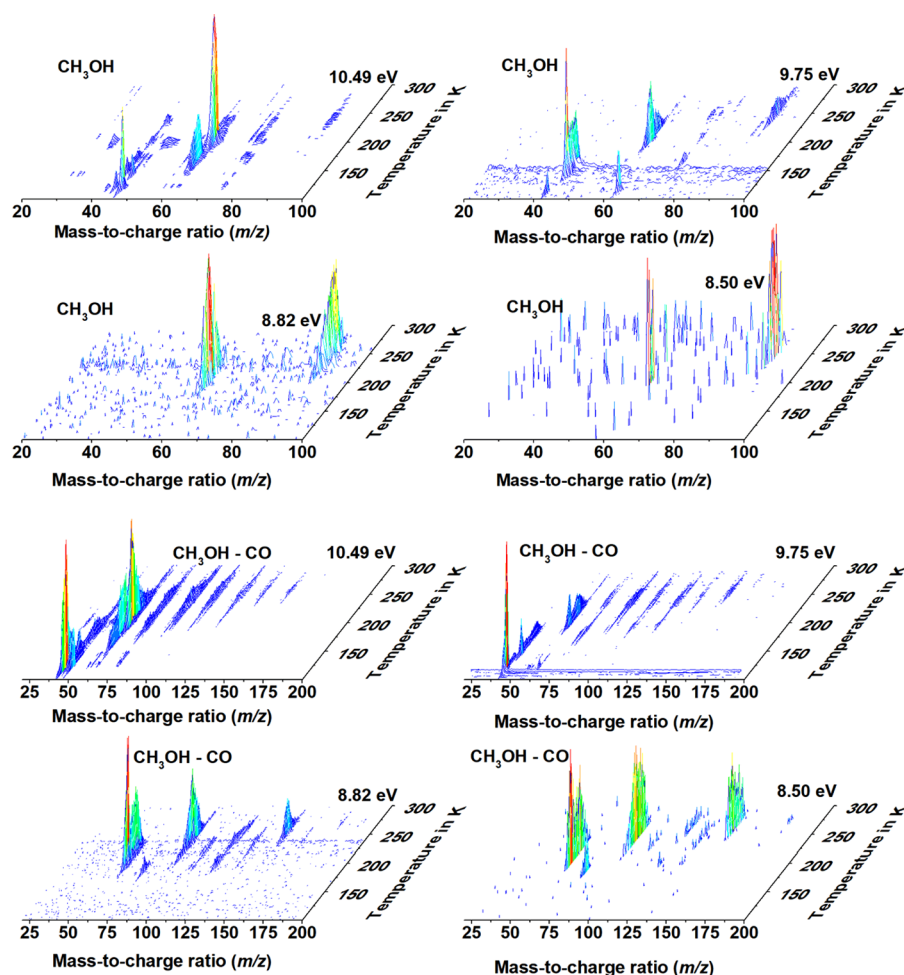


Figure 2. Temperature-dependent time-of-flight mass spectra recorded at different photon energies for pure methanol ices (top four panels) and methanol–carbon monoxide ices (bottom four panels) after electron irradiation. Data at 10.49 eV were taken from ref 56.

the ice–metal interface. In pure methanol ices, the dose was found to be 5.3 ± 0.8 eV molecule⁻¹, whereas in the mixed ice, the dose corresponded to 4.9 ± 0.8 eV molecule⁻¹ and 4.2 ± 0.7 eV molecule⁻¹ for methanol and carbon monoxide, respectively (Table S2). For the temperature-programmed desorption, a cartridge heater interfaced to a temperature controller was used to heat the sample at a constant ramp of 0.5 K min⁻¹. Subliming species were ionized using a pulsed, laser-based, tunable VUV source for soft, ideally fragment-free ionization. The resulting cations were then collected by a TOF-spectrometer (Jordan TOF products Inc.) and analyzed according to their arrival time at the micro channel plate detector. Corresponding mass-to-charge ratios were assigned using a previously recorded calibration curve³⁰ as the starting condition for a fit routine fitting a fifth-order polynomial to the peaks in the mass spectrum to compensate for slight deviations of distance between sample and spectrometer. Tunable vacuum ultraviolet (VUV) radiation was generated by (non)resonant four-wave mixing in noble gases.³⁷ Pulsed lasers operating at a repetition rate of 30 Hz were synchronized to a pulsed valve operated at a backing pressure of 2 atm. To generate 10.49 eV, the frequency-tripled output of a Nd:YAG laser (Spectra Physics QuantaRay Pro 250-30, 354.6 nm) was focused into a xenon gas jet produced by the pulsed valve to achieve frequency tripling by nonresonant four-wave mixing. Photon energies of 9.75 and 8.50 eV were generated by resonant four-wave difference frequency mixing ($2\omega_1 - \omega_2$) in krypton, whereas 8.82 and 8.05 eV were produced in xenon gas. For these wavelengths, the outputs of two tunable dye lasers (Sirah Lasertechnik, Cobra-Stretch) pumped by two electronically synchronized Nd:YAG lasers (Spectra Physics QuantaRay Pro 250-30 and 270-30) were overlapped spatially and temporally inside the gas jet produced by the pulsed valve. The

generated VUV light was separated from the laser beams using a biconvex lithium fluoride lens in an off-axis geometry on a translation stage, only allowing the desired wavelength to pass through an aperture into the main experimental chamber. Behind the aperture, the transmitted beam passes the sample at a distance of 2 mm to ionize subliming molecules and subsequently illuminates a faraday cup held at a voltage of 300 V to monitor the VUV flux. For each experiment, the recorded TPD profiles were normalized to the VUV flux to minimize the influence of fluctuations on the profiles. Wavelengths and dyes used for each photon energy are summarized in Table S3. The exploitation of interstellar analogue ices represents a validated strategy and very first step as verified by Ehrenfreund et al.³⁸

COMPUTATIONAL DETAILS

All computations were carried out with Gaussian 16, Revision A.03.³⁹ For geometry optimizations and frequency computations, the density functional theory (DFT) B3LYP functional^{40–42} was employed utilizing the Dunning correlation-consistent split valence basis set cc-pVTZ.⁴³ Based on these geometries, the corresponding frozen-core coupled cluster^{44–47} CCSD(T)/cc-pVDZ, CCSD(T)/cc-pVTZ, and CCSD(T)/cc-pVQZ single point energies were computed and extrapolated to complete basis set limit⁴⁸ CCSD(T)/CBS with B3LYP/cc-pVTZ zero-point vibrational energy (ZPVE) corrections. The adiabatic ionization energies were computed by taking the ZPVE corrected energy difference between the neutral and ionic species that correspond to similar conformations. At this level of

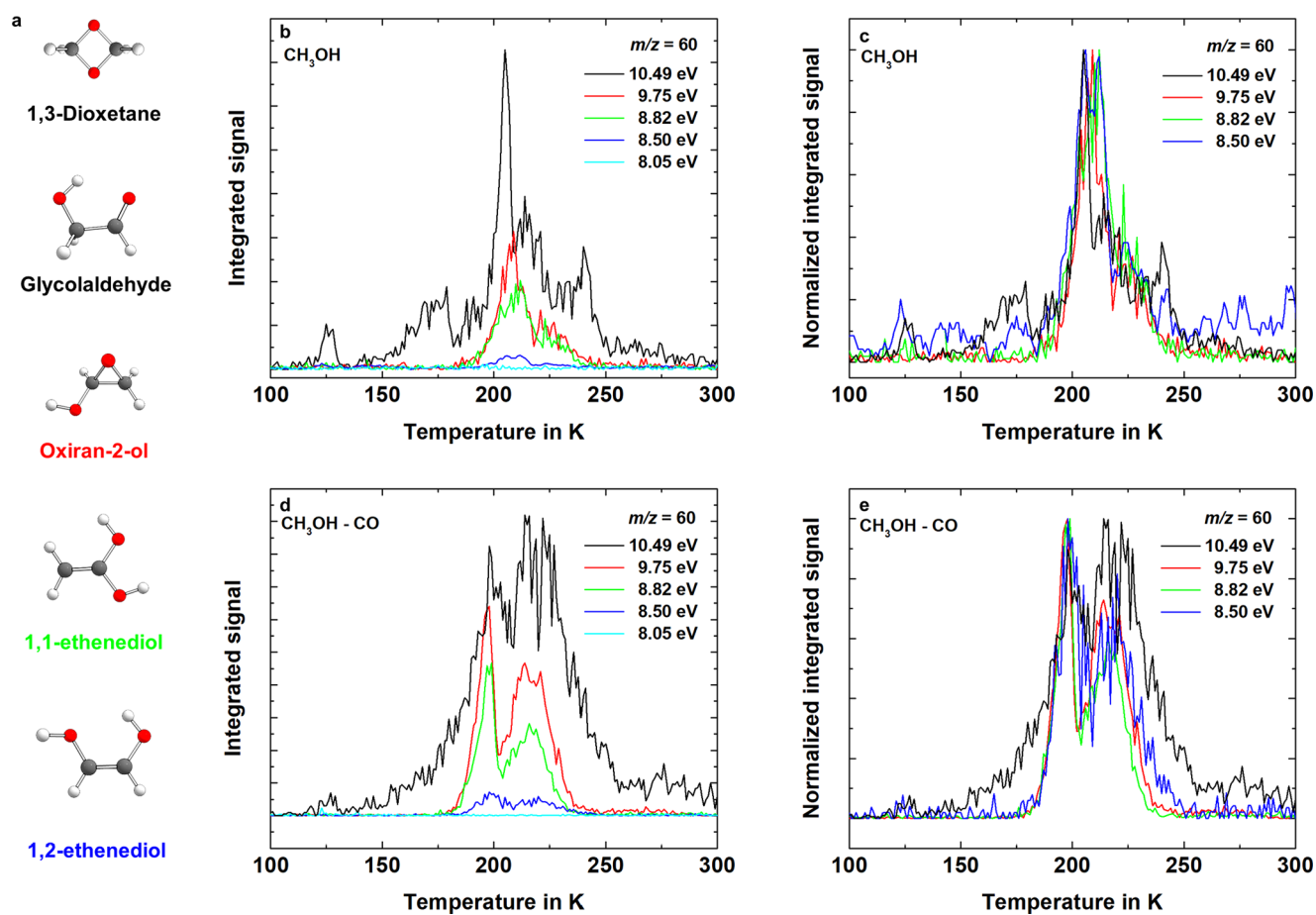


Figure 3. TPD profiles of $C_2H_4O_2$ ($m/z = 60$). Isomers detectable at the photon energies used based on their ionization energies (Table S7) (a). The caption colors correspond to the lowest photon energy at which the isomer is detectable in the experiments. Profiles were recorded for pure methanol ices (b and c) and methanol–carbon monoxide ices (d and e) at different photon energies after electron irradiation. The right panels show normalized data to compare desorption profiles. Data at 10.49 eV were taken from ref S6.

theory, typical uncertainties of relative energies are around 4 kJ mol^{-1} . Calculations performed for a small subset of the molecules using the computationally more expensive augmented basis sets at the same zeta level revealed that they did not affect the ionization energies to the significant figures reported and only had a marginal effect on the relative energies ($<2.5 \text{ kJ mol}^{-1}$). Therefore, the cc-pVTZ basis set is sufficient for the present purposes and was utilized for all molecules to save computation time without sacrificing the required accuracy. Furthermore, the difference in deuterated and nondeuterated isotopologues in the ZPVE is marginal ($<0.01 \text{ eV}$) so we can exploit the ZPVEs of nondeuterated isotopologues for the determination of ionization energies.

RESULTS

Infrared Spectroscopy. Infrared spectra of pure methanol (CH_3OH) and methanol (CH_3OH)–carbon monoxide (CO) ices were recorded before, during, and after the exposure to energetic electrons to monitor changes in the chemical composition of the ices. A comprehensive overview of the absorption features detected is presented in Tables S4 and S5 for pure methanol and methanol–carbon monoxide ices, respectively. In both pristine systems, absorption features can be associated with the reactants (Figures S1 and S2; black labels). Methanol is identified by its broad OH stretch (ν_1 , $3600\text{--}3020 \text{ cm}^{-1}$), the symmetric stretching modes of the methyl group (ν_9 ,

2950 cm^{-1} ; ν_3 , 2825 cm^{-1}), the CH_3 rocking mode (ν_{11} , 1040 cm^{-1}), and the CO stretch (ν_8) at 1026 cm^{-1} . In the methanol–carbon monoxide ice, an additional absorption can be assigned to the CO stretching mode of carbon monoxide (2136 cm^{-1}).

After the irradiation of the pure methanol ices (Figure S1, Table S4), several new absorptions emerged (red labels). The most prominent features are attributed to the carbonyl ($C=O$) stretch of formaldehyde (ν_2 , 1726 cm^{-1}). This assignment is further supported by the detection of its CH_2 scissoring (ν_3 , 1508 cm^{-1}) and CH_2 bending modes (ν_6 , 1177 cm^{-1}).⁴⁹ On the basis of previous studies, absorptions linked to methyl formate ($HCOOCH_3$; ν_{14} , 1718 cm^{-1}) and glycolaldehyde (ν_{14} , 1750 cm^{-1} ; $2\nu_6$, 1700 cm^{-1}) can be identified.⁵⁰ Furthermore, carbon monoxide can be probed via its stretching mode (ν_1 , 2134 cm^{-1}), carbon dioxide (CO_2) via its $C=O$ asymmetric stretch (ν_3 , 2340 cm^{-1}) and the bending mode (ν_2 , 667 cm^{-1}), and methane (CH_4) via its deformation mode (ν_4 , 1302 cm^{-1}). In addition to the aforementioned closed shell molecules, the formyl ($HCO\bullet$, 7; ν_3 , 1844 cm^{-1} ; ν_2 , 1092 cm^{-1})⁵¹ and hydroxymethyl ($CH_2OH\bullet$, 8; ν_6 , 1192 cm^{-1})⁵¹ radicals are observed at abundances of $(2.4 \pm 0.6) \times 10^{14}$ molecules) and $(1.4 \pm 0.2) \times 10^{15}$ molecules), respectively, based on their measured (formyl)⁵² and calculated (hydroxymethyl)⁵³ absolute absorption intensities. In the methanol–carbon monoxide ice mixtures (Figure S2), the same molecules and radicals formed as in the pure methanol ices. The abundance of formyl

radicals increased to $(2 \pm 1) \times 10^{15}$ molecules, whereas hydroxymethyl decreased to $(8 \pm 2) \times 10^{15}$ molecules. It is important to highlight that in complex mixtures such as those formed in the present studies, infrared spectroscopy primarily only identifies *functional groups* of newly formed organic molecules, but not necessarily *individual molecules*. Functional groups of organics such as 3, e.g., stretching and bending modes of hydroxyl groups (OH) and of carbon–carbon double bonds (C=C), often overlap with other species and cannot be uniquely assigned to an individual molecule (Table S6). Therefore, to identify 3 in these complex mixtures, an alternative, *isomer-selective* technique is required.

PI-ReToF-MS. Individual structural isomers are identified by exploiting soft photoionization reflectron time-of-flight mass spectrometry (PI-ReToF-MS) coupled with temperature-programmed desorption (TPD) of the newly formed molecules.⁵⁴ This technique allows us to distinguish molecules based on their mass-to-charge ratios, their desorption temperatures and profiles, and their distinct ionization energies. Temperature-dependent mass spectra recorded at different photon energies are displayed in Figure 2 to provide an overview of the mass-to-charge ratios of all product molecules. The adiabatic ionization energies (IE) for the C₂H₄O₂ isomers are compiled in Table S7 (IE_{calc}) and compared to experimentally determined values whenever available (IE_{exp}). To gauge the accuracy of the computed adiabatic ionization energies, adiabatic ionization energies for organic molecules with known experimental ionization energies were calculated (Table S8). These benchmarks suggest that the computed adiabatic ionization energies are accurate within $-0.06/+0.11$ eV (Supporting Information). It should be noted that the electric field of the ionizer optics of the ReToF decreases the ionization energies by 0.03 eV.⁵⁵ Overall, by systematically tuning the ionization energies from 10.49 to 8.05 eV, this approach provides compelling evidence on the first bottom-up formation and detection of 1,2-ethenediol.

At a photon energy of 10.49 eV, all C₂H₄O₂ isomers considered here with the exception of acetic acid (IE_{exp} = 10.65 ± 0.02 eV) and methyl formate (IE_{exp} = 10.835 eV), which are not a subject of this study, can be ionized (Figure 3a, Table S7).^{30,56} The relevant TPD traces at $m/z = 60$ are shown in Figure 3 for pure methanol ices (top row, black line) and methanol–carbon monoxide ices (bottom row, black line). Several desorption peaks are visible for $m/z = 60$.³⁰ Extensive isotopic substitution experiments assigned the sublimation event at 125 K to C₃H₈O isomers.⁵⁶ Furthermore, on the basis of the desorption profile, the sublimation event at 235 K has been ascribed to photofragmentation of glycerol with an appearance energy of 9.9 eV for the C₂H₄O₂⁺ fragment.⁵⁷ The remaining sublimation events were associated with C₂H₄O₂ isomers based on experiments with isotopic substitutions.^{30,56} Control experiments were also conducted in a fashion similar to that of the actual experiments but without exposing the ices to energetic electrons in the TPD phase. No ion counts were observed at the aforementioned masses, revealing that the observed ion counts are linked to the energetic processing of the ices.

Tuning the photon energy down to 9.75 eV (Figure 3, red line), glycolaldehyde (IE_{exp} = 9.95 ± 0.05 eV) as well as 1,3-dioxetane (IE_{calc} = 10.08 eV) cannot be ionized anymore. In both systems, the TPD profiles at $m/z = 60$ recorded at 9.75 eV differ significantly from the TPD profiles obtained at 10.49 eV. The sublimation onset shifts from 135 K to 175 K, and the sublimation event at 235 K vanishes as well; this is in accordance

with the reported appearance energy of the C₂H₄O₂⁺ fragment of glycerol.⁵⁷ The remaining two distinct sublimation events at 210 K and 225 K (methanol) and 198 K and 217 K (methanol–carbon monoxide) can therefore only be linked to either the target compound 1,2-ethenediol (IE_{calc} = 8.16–8.41 eV), 1,1-ethenediol (IE_{calc} = 8.58–8.68 eV), or oxiran-2-ol (IE_{calc} = 8.93 eV) (Table S7).

To exclude the latter isomer, we tuned the photon energy to 8.82 eV (Figure 3, green line). This led to an overall reduction of the ion counts. However, the normalized TPD traces (Figure 3, right panels) clearly show that the desorption profiles do not change. This finding indicates that oxiran-2-ol does not contribute to the ion signal at $m/z = 60$. Only 1,2-ethenediol (IE_{calc} = 8.16–8.41 eV) and/or 1,1-ethenediol (IE_{calc} = 8.58–8.68 eV) remain as possible candidates for the ion counts at $m/z = 60$ at 8.82 eV.

To discriminate 1,2-ethenediol (IE_{calc} = 8.16–8.41 eV) from 1,1-ethenediol (IE_{calc} = 8.58–8.68 eV), we tuned the photon energy down to 8.50 eV (Figure 3, blue line). At this photon energy, the only C₂H₄O₂ isomer that can be ionized is 1,2-ethenediol with computed ionization energies of IE_{calc} = 8.16–8.41 eV. As evident from the normalized TPD traces, the desorption profiles remain similar to those at a higher photon energy of 8.82 eV. Therefore, it can be concluded that both desorption events can only be due to 1,2-ethenediol.

How can we explain the observation of two sublimation peaks at 198 K and 216 K? These distinct events could be either due to codesorption with ethylene glycol ((CH₂OH)₂, 9) sublimating at around 200 K³⁰ or might be the result of two (groups of) different configurational isomers with the hydroxyl groups located in either *E* or *Z* configuration. This leads to different polarities ranging from 0 D for 3c to 2.36 D for 3d, with more polar molecules resulting in increased desorption temperatures.²⁸

Exploiting previously determined calibration factors,⁵⁸ the signal at 8.50 eV can be used to quantify 1,2-ethenediol in both ices in dependence of the (unknown) photoionization cross-section. According to this analysis, in the pure methanol ice, $(1.3 \pm 0.2) \times 10^{14}$ /photoionization cross-section [Mb] molecules are formed, whereas $(9 \pm 1) \times 10^{14}$ /photoionization cross-section [Mb] molecules are formed in the mixed ice. With a cross-section of 1–10 Mb, which are typical values within the first 200–300 meV of the ionization threshold, these values correspond to the formation of $(1.3 \pm 0.2) \times 10^{13-14}$ and $(9 \pm 1) \times 10^{13-14}$ molecules in the pure methanol and methanol–carbon monoxide ice mixtures, respectively. Finally, we also conducted an experiment at 8.05 eV (Figure 3 (cyan line); Figure S3), which is below the ionization energy of any C₂H₄O₂ isomer. No ion signal at $m/z = 60$ is observable anymore.

DISCUSSION

Reaction Pathways in CH₃OH Ice. With the identification of 1,2-ethenediol, we shift our focus to elucidating a possible reaction mechanism to its formation. A comparison of the molecular structures of the reactants with 1,2-ethenediol suggests that at least two methanol molecules are required in the formation. Subjected to energetic electrons, methanol can decompose via atomic hydrogen loss from the methyl and from the hydroxyl group forming the hydroxymethyl (•CH₂OH) and methoxy (CH₃O•) radical, respectively, of which only the hydroxymethyl radical has been identified in the IR spectra (Figures S1 and S2, Tables S4 and S5).⁵⁰ Higher order decomposition products are formaldehyde, hydroxymethylene

(H–C̣–OH), and carbon monoxide. To decipher the reaction pathway(s) of 1,2-ethenediol in methanol ices, we exploited partially deuterated methanol-OD (CH₃OD), allowing us to distinguish reaction pathways involving hydrogen loss at the methyl and the hydroxy group, respectively. The photon energy for the photoionization of the subliming species was selected as 8.50 eV so that only 1,2-ethenediol can be ionized (*vide infra*). The strongest ion signal was detected at $m/z = 62$ (green line, Figure 4a); this signal corresponds to an isotopologue of 1,2-

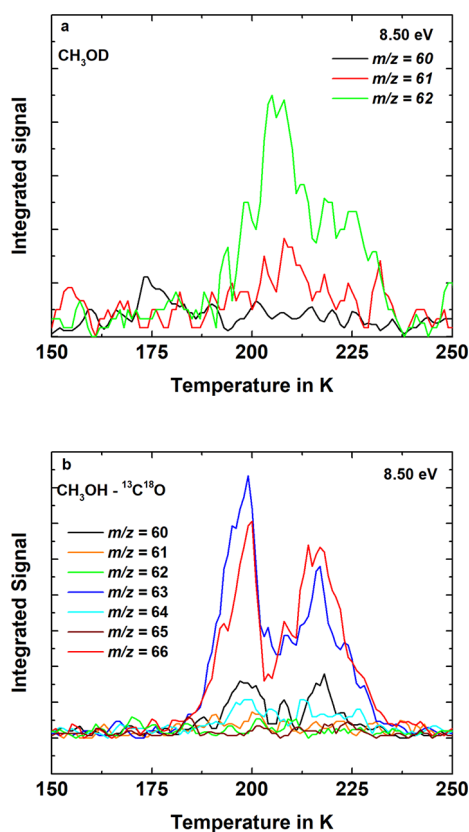
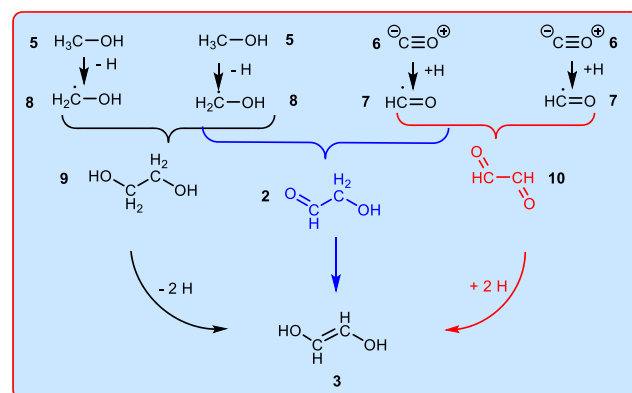


Figure 4. TPD profiles of isotopically labeled products. C₂H₄O₂ ($m/z = 60$), C₂H₃DO₂ ($m/z = 61$), and C₂H₂D₂O₂ ($m/z = 62$) in pure methanol-OD (CH₃OD) ices after electron irradiation recorded at 8.50 eV (a). C₂H₄O₂ ($m/z = 60$), ¹³C¹²CH₄O₂ ($m/z = 61$), C₂H₄¹⁸O¹⁶O ($m/z = 62$), ¹³C¹²CH₄¹⁸O¹⁶O ($m/z = 63$), ¹³C₂H₄¹⁸O¹⁶O ($m/z = 64$), ¹³C¹²CH₄¹⁸O₂ ($m/z = 65$), and ¹³C₂H₄¹⁸O₂ ($m/z = 66$) in methanol–carbon monoxide-¹³C¹⁸O ices after electron irradiation recorded at 8.50 eV (b).

ethenediol with the molecular formula C₂H₂D₂O₂. No signal was detected at $m/z = 60$ (black line, Figure 4a), suggesting that no isotopologue with the molecular formula C₂H₄O₂ was formed. These findings reveal that in methanol-OD (CH₃OD) ices, the formation of 1,2-ethenediol may involve three pathways: the dimerization of two hydroxycarbenes-OD (H–C̣–OD; 31 amu), the recombination of two hydroxymethyl-OD radicals (•CH₂OD; 32 amu) to form ethylene glycol-*d*₂ (DOCH₂CH₂OD; 64 amu) followed by the loss of two hydrogens, and/or insertion of hydroxymethylene-OD (H–C̣–OD; 31 amu) into the C–H bond of a neighboring methanol-OD (33 amu) followed by loss of two hydrogens (Figure S4). The dimerization of hydroxymethylene-*d*₁ could directly yield 1,2-ethenediol; however, according to electronic structure calculations, hydroxymethylene does not undergo dimerization because of a theoretically favored double hydrogen

transfer reaction to yield a complex of two formaldehyde molecules but not 1,2-ethenediol.⁵⁹ Furthermore, carbenes exhibit a high reactivity with closed shell molecules such as found in the surrounding ice matrix,^{10,59} or, in the case of hydroxycarbenes, they can rearrange by tunneling to form closed-shell molecules.⁶⁰ Consequently, for the dimerization of hydroxymethylene, two highly reactive carbenes need to be formed adjacent to each other in a favorable reaction geometry. Therefore, hydroxymethylene will presumably be quenched instantly by the methanol matrix surrounding it, and a reaction with a methanol molecule may yield ethylene glycol-*d*₂ (DOCH₂CH₂OD; 64 amu). Therefore, our results suggest that in methanol ices, ethylene glycol, accessed either by recombination of two hydroxymethyl radicals or via C–H insertion reaction of hydroxymethylene with methanol, represents a critical intermediate in the formation of 1,2-ethenediol (Figure S4, Scheme 1). Ethylene glycol was detected

Scheme 1. Derived Reaction Pathways in Methanol–Carbon Monoxide Ices Leading to the Formation of 1,2-Ethenediol^a



^aThe colors of pathways correspond to the color code used in Figure 4. *E/Z* isomers are omitted for clarity.

via PI-ReTOF-MS in electron-exposed methanol ices;¹³ the hydroxymethyl radical was observed in the infrared spectra (Table S4). The low signal of ion counts at $m/z = 61$ (red line in Figure 4a) can be accounted for by H/D exchange during deposition as seen by the residual OH stretching signal in the infrared spectrum taken after deposition (Figure S5).

Further support for the inferred reaction pathway is found in a computational study by Simons et al., who calculated reaction rates and branching ratios for all reactions occurring during hydrogenation of carbon monoxide.⁶¹ These calculations confirm that ethylene glycol can form from two hydroxymethyl radicals. Furthermore, the radical intermediate •CHOHCH₂OH was calculated to be the main dehydrogenation pathway of ethylene glycol.⁶¹ As their model only included hydrogen interactions rather than ionizing radiation, further dehydrogenation of •CHOHCH₂OH was not observed, as the attachment of a hydrogen atom is favored over hydrogen-induced abstraction. In contrast, the energetic electrons employed in our study could induce further dehydrogenation and thus lead to the formation of 1,2-ethenediol.

To further confirm this reaction pathway, we deposited a 600 nm thick ice of pure ethylene glycol and irradiated it with the same number of impinging electrons as for the methanol and methanol–carbon monoxide ices. As in the previous experiments, using a photon energy of 8.50 eV allows us to exclude any

other possible molecule at $m/z = 60$. Figure S6 shows the resulting desorption profile, clearly identifying 1,2-ethenediol as a product of ethylene glycol irradiation. Because under the reaction conditions in our experiments $11 \pm 2\%$ ($(6 \pm 1) \times 10^{16}$ molecules) of the methanol is converted to ethylene glycol,¹³ the inferred pathway seems the most plausible for 1,2-ethenediol formation from methanol.

Reaction Pathways in CH₃OH–CO Ices. The mechanisms of formation of 1,2-ethenediol were traced by exploiting ¹³C¹⁸O:CH₃OH ices and tracing the isotopically substituted counterparts of 1,2-ethenediol based on distinct m/z ratios at a photon energy of 8.50 eV. At this energy, only 1,2-ethenediol can be ionized, and no fragment ions were observed. Contingent upon distinct numbers of ¹³C and ¹⁸O incorporated in isotopically labeled 1,2-ethenediol, mass-to-charge ratios between 60 (HOCHCHOH; no incorporation of ¹³C¹⁸O) and 66 (H¹⁸O¹³CH¹³CH¹⁸OH; incorporation of two ¹³C¹⁸O with methanol supplying hydrogen atoms) are possible. The TPD traces of mass-to-charge ratios from 60 to 66 are shown in Figure 4b. Apart from $m/z = 61$, $m/z = 62$, and $m/z = 65$, ion signals are detected for all relevant channels and display identical desorption profiles (Figure 4b). The detection of signal at $m/z = 60$, 63, and 66 indicates that reactions leading to 1,2-ethenediol can involve either two methanol molecules (vide supra, pathway 1 in Figure S7), one methanol molecule and one carbon monoxide-¹³C¹⁸O molecule, or two carbon monoxide-¹³C¹⁸O molecules with methanol only supplying the hydrogen atoms with branching ratios of $10 \pm 2\%$, $45 \pm 5\%$, and $45 \pm 5\%$, respectively. Based on the relative strength compared to $m/z = 66$ ($<10\%$), the signal at $m/z = 64$ can entirely be accounted for by the isotopic impurity of carbon monoxide-¹³C¹⁸O (99% ¹³C, 95% ¹⁸O) and therefore does not reveal additional pathways.

Considering that both the formyl and the hydroxymethyl radical were detected infrared spectroscopically, the most plausible reaction pathway for reactions involving one methanol and one ¹³C¹⁸O molecule ($m/z = 63$) is the barrierless recombination of a hydroxymethyl radical with a formyl radical to form glycolaldehyde⁵⁰ followed by radiolytically induced enolization to 1,2-ethenediol (pathway 2 in Figure S7; Scheme 1). The double hydrogen shift for the enolization of glycolaldehyde has a calculated barrier height of 277 kJ mol^{-1} at the G3X-K level of theory,⁶² which is similar to that for the enolization of acetaldehyde to vinyl alcohol (277 kJ mol^{-1}).⁶³ Recently, Kleimeier and Kaiser have demonstrated that enolization of acetaldehyde can be induced by 5 keV electron irradiation as proxy for galactic cosmic rays by inter- and intramolecular hydrogen shifts, indicating that this pathway is feasible for the enolization of aldehydes.⁶⁴ Based on the infrared spectroscopic detection of the formyl radical, the most plausible reaction leading to 1,2-ethenediol in reactions involving two ¹³C¹⁸O molecules ($m/z = 66$) is the dimerization of formyl to glyoxal (HCOCHO, 10) followed by reduction through addition of two (suprathermal) hydrogen atoms (pathway 3 in Figure S7; Scheme 1). An experimental study by Chuang et al.⁶⁵ as well as surface carbon monoxide hydrogenation studies by Fedoseev et al.⁶⁶ indicate that glyoxal formation from formyl and subsequent hydrogenation are the dominant contributors to glycolaldehyde as well as ethylene glycol formation. These results are consistent with a computational modeling study by Simons et al.⁶¹ who calculated a reasonably high reaction rate for the hydrogenation of glyoxal with branching ratios of 33% for the formation of the OCHCH₂O• radical and 0.033% for the

formation of the HOCHCHO• radical. However, due to the high residual energy of hydrogen atoms in the ice after ionization with 5 keV electrons, the branching ratio might be different in our experiments and be more in favor of the HOCHCHO• radical, which can directly be hydrogenated to 1,2-ethenediol. Woods et al. calculated the barrier to addition for glyoxal to form the OCHCH₂O• radical to be 9.18 kJ mol^{-1} , which can easily be overcome by the excess energy of the suprathermal hydrogens abstracted from the methanol molecules in our experiments.

Further support for this reaction pathway was found by Maity et al. in an extensive study of molecule formation in electron-irradiated methanol–carbon monoxide ices.⁵⁶ Their experiments with different isotopic substitutions clearly show that glyoxal formation in these ice mixtures is dominated by reactions including two carbon monoxide molecules rather than one methanol and one carbon monoxide molecule. However, due to a lack of isomer-selective detection methods, none of the experimental studies conducted prior to this work could discriminate glycolaldehyde from its enol isomer 1,2-ethenediol.

CONCLUSION

Our study provides compelling evidence on the formation and isomer-selective mass spectrometric identification of 1,2-ethenediol in ice consisting of methanol and in methanol–carbon monoxide mixtures, respectively. Exploiting isotopically labeled ices, at least three reaction mechanisms could be untangled involving barrierless radical–radical recombinations, (de)hydrogenation, and keto–enol isomerization. This study represents the proof-of-concept on the formation of high-energy isomers of ubiquitous ketones and aldehydes, enols, in interstellar analogue ices composed of methanol and mixtures of methanol and carbon monoxide followed by their detection in the gas phase upon sublimation. Interstellar ices containing carbon monoxide and methanol at levels of up to 50% and 30%, respectively, have been observed toward high- and low-mass star-forming regions.^{31,32} Therefore, 1,2-ethenediol could be searched for in the gas phase of the interstellar medium after sublimation from the grains utilizing telescopes such as ALMA.

Laboratory studies exposing interstellar model ices to ionizing radiation have demonstrated that the abiotic formation of biologically relevant molecules is feasible under interstellar conditions. This implies that key biological compounds such as sugars might form on ice-coated interstellar grains, the raw material for solar systems, by energetic processing in cold molecular clouds at temperatures as low as 10 K. Those organics are eventually incorporated into parent bodies of meteorites which can partially survive entry into the atmosphere of planets like Earth.¹² In fact, carbohydrates that were detected in energetically processed interstellar model ices in laboratory experiments^{18,19} were also found in meteorite samples.^{14,15}

Overall, as interstellar ices are dominated by water,³¹ water-assisted chemical reactions are feasible, similar to those in aqueous solutions as revealed computationally by Chen and Woon.⁶⁷ As formaldehyde has firmly been detected in interstellar ices, water-assisted (cosmic ray driven) aldol reactions between formaldehyde and 1,2-ethenediol seem conceivable in interstellar ices.¹⁸ In a computational study of aldol reactions, Kua et al. calculated that the enolization of glycolaldehyde to its enol is endergonic by 39 kJ mol^{-1} with the barrier to water-assisted enolization amounting to 88 kJ mol^{-1} ;⁶⁸ this indicates that 1,2-ethenediol can only form through nonequilibrium reactions for which the energy is supplied by the energetic processing of the ices or by tunneling processes.

Once formed, the barrier for the aldol reaction to form glyceraldehyde from glycolaldehyde and 1,2-ethenediol (24 kJ mol⁻¹) can easily be overcome under typical formose reaction conditions at elevated temperatures on Earth but probably not under interstellar ice thermal equilibrium conditions at low temperatures.⁶⁸ However, these reactions can either proceed by energetic processing through galactic cosmic rays or photons, or by quantum tunneling-assisted/dominated reactions to yield the simplest chiral sugar glyceraldehyde. Indeed, glyceraldehyde along with its thermodynamically preferred isomerization product dihydroxyacetone has been detected in meteorite samples⁶⁹ and in the organic residues of photolyzed methanol and water-containing ice mixtures by Meinert et al.¹⁸ The authors consequently concluded that the detected reaction products in the residues such as sugars, sugar alcohols, sugar acids, and branched chain molecules are indicative of a formose-type reactivity in their water-dominated interstellar model ices. In contrast to their interpretation that formaldehyde and glycolaldehyde are the main reactants, our results clearly indicate that the much more reactive 1,2-ethenediol also forms in such irradiated ices. Therefore, it should be considered as one of the key intermediates in the formation of sugars besides hydroxymethylene (H–C̈–OH), which has been shown to barrierlessly react with formaldehyde to form glycolaldehyde and in an iterative fashion glyceraldehyde.¹⁰

These results provide insight into an additional pathway toward sugar formation in the interstellar medium, comets, and asteroids apart from the mechanochemical pathway unraveled by Haas et al.,⁹ thereby indicating a wider range of conditions under which sugars can form to ultimately be delivered to planets where life could evolve.

On a final note, it is important to consider that no simulation experiment can replicate the chemical complexity and diverse radiation environment of the interstellar medium concurrently; interstellar ices are exposed to not only galactic cosmic rays (GCRs) but also simultaneously to ultraviolet (UV) photons. UV photons penetrate only the first few icy layers of the grains, whereas GCRs pass through the icy mantle. Consequently, simulation experiments have to be conducted first with well-defined model ices as carried out here to advance the understanding of the fundamental processes leading to key organics such as enols in the ices thus eliminating the gap between observational and laboratory data that existed for decades, bringing us closer to eventually predicting where in the galaxy molecular precursors linked to the origins of life might exist.

■ ASSOCIATED CONTENT

SI Supporting Information

The Supporting Information is available free of charge at <https://pubs.acs.org/doi/10.1021/jacs.1c07978>.

Error estimation of computed ionization energies, H₃OH–CO ratio determination, Figures S1–S7, Tables S1–S8, and cartesian coordinates for selected structures of C₂H₄O₂ (PDF)

■ AUTHOR INFORMATION

Corresponding Authors

Ralf I. Kaiser – Department of Chemistry, University of Hawaii at Mānoa, Honolulu, Hawaii 96822, United States; W. M. Keck Laboratory in Astrochemistry, University of Hawaii at Mānoa, Honolulu, Hawaii 96822, United States;

orcid.org/0000-0002-7233-7206; Email: ralfk@hawaii.edu

N. Fabian Kleimeier – Department of Chemistry, University of Hawaii at Mānoa, Honolulu, Hawaii 96822, United States; W. M. Keck Laboratory in Astrochemistry, University of Hawaii at Mānoa, Honolulu, Hawaii 96822, United States;

orcid.org/0000-0003-1767-897X; Email: nfk@hawaii.edu

André K. Eckhardt – Department of Chemistry, Massachusetts Institute of Technology, Cambridge, Massachusetts 02139, United States; orcid.org/0000-0003-1029-9272; Email: ake05@mit.edu

Complete contact information is available at: <https://pubs.acs.org/10.1021/jacs.1c07978>

Author Contributions

The manuscript was written through contributions of all authors. All authors have given approval to the final version of the manuscript.

Notes

The authors declare no competing financial interest.

■ ACKNOWLEDGMENTS

Financial support from the U.S. National Science Foundation (AST-1800975) is greatly acknowledged (N.F.K, R.I.K.). The experimental setup was financed by the W. M. Keck Foundation. N.F.K. acknowledges funding from the Deutsche Forschungsgemeinschaft (DFG, German Research Foundation) for a postdoctoral fellowship (KL 3342/1-1). A.K.E. thanks the Alexander von Humboldt Foundation for a Feodor Lynen Research Fellowship.

■ REFERENCES

- (1) Butlerow, A. Bildung einer zuckerartigen Substanz durch Synthese. *Justus Liebigs Ann. Chem.* **1861**, *120*, 295.
- (2) Breslow, R. On the mechanism of the formose reaction. *Tetrahedron Lett.* **1959**, *1*, 22.
- (3) Appayee, C.; Breslow, R. Deuterium studies reveal a new mechanism for the formose reaction involving hydride shifts. *J. Am. Chem. Soc.* **2014**, *136*, 3720.
- (4) Cheng, L.; Doubleday, C.; Breslow, R. Evidence for tunneling in base-catalyzed isomerization of glyceraldehyde to dihydroxyacetone by hydride shift under formose conditions. *Proc. Natl. Acad. Sci. U. S. A.* **2015**, *112*, 4218.
- (5) Kua, J.; Galloway, M. M.; Millage, K. D.; Avila, J. E.; De Haan, D. O. Glycolaldehyde monomer and oligomer equilibria in aqueous solution: comparing computational chemistry and NMR data. *J. Phys. Chem. A* **2013**, *117*, 2997.
- (6) Teichert, J. S.; Kruse, F. M.; Trapp, O. Direct Prebiotic Pathway to DNA Nucleosides. *Angew. Chem., Int. Ed.* **2019**, *58*, 9944.
- (7) Ricardo, A.; Carrigan, M. A.; Olcott, A. N.; Benner, S. A. Borate minerals stabilize ribose. *Science* **2004**, *303*, 196.
- (8) Ritson, D.; Sutherland, J. D. Prebiotic synthesis of simple sugars by photoredox systems chemistry. *Nat. Chem.* **2012**, *4*, 895.
- (9) Haas, M.; Lamour, S.; Christ, S. B.; Trapp, O. Mineral-mediated carbohydrate synthesis by mechanical forces in a primordial geochemical setting. *Communications Chemistry* **2020**, *3*, 140.
- (10) Eckhardt, A. K.; Linden, M. M.; Wende, R. C.; Bernhardt, B.; Schreiner, P. R. Gas-phase sugar formation using hydroxymethylene as the reactive formaldehyde isomer. *Nat. Chem.* **2018**, *10*, 1141.
- (11) Eckhardt, A. K.; Wende, R. C.; Schreiner, P. R. 1,3-Dioxolane-4-ol hemiacetal stores formaldehyde and glycolaldehyde in the gas-phase. *J. Am. Chem. Soc.* **2018**, *140*, 12333.
- (12) Arumainayagam, C. R.; Garrod, R. T.; Boyer, M. C.; Hay, A. K.; Bao, S. T.; Campbell, J. S.; Wang, J.; Nowak, C. M.; Arumainayagam, M.

- R.; Hodge, P. J. Extraterrestrial prebiotic molecules: photochemistry vs. radiation chemistry of interstellar ices. *Chem. Soc. Rev.* **2019**, *48*, 2293.
- (13) Kaiser, R. I.; Maity, S.; Jones, B. M. Synthesis of prebiotic glycerol in interstellar ices. *Angew. Chem., Int. Ed.* **2015**, *54*, 195.
- (14) Cooper, G.; Kimmich, N.; Belisle, W.; Sarinana, J.; Brabham, K.; Garrel, L. Carbonaceous meteorites as a source of sugar-related organic compounds for the early earth. *Nature* **2001**, *414*, 879.
- (15) Furukawa, Y.; Chikaraishi, Y.; Ohkouchi, N.; Ogawa, N. O.; Glavin, D. P.; Dworkin, J. P.; Abe, C.; Nakamura, T. Extraterrestrial ribose and other sugars in primitive meteorites. *Proc. Natl. Acad. Sci. U. S. A.* **2019**, *116*, 24440.
- (16) Kleimeier, N. F.; Eckhardt, A. K.; Schreiner, P. R.; Kaiser, R. I. Interstellar Formation of Biorelevant Pyruvic Acid (CH_3COCO). *Chem.* **2020**, *6*, 3385.
- (17) Cooper, G.; Reed, C.; Nguyen, D.; Carter, M.; Wang, Y. Detection and formation scenario of citric acid, pyruvic acid, and other possible metabolism precursors in carbonaceous meteorites. *Proc. Natl. Acad. Sci. U. S. A.* **2011**, *108*, 14015.
- (18) Meinert, C.; Myrgorodska, I.; de Marcellus, P.; Buhse, T.; Nahon, L.; Hoffmann, S. V.; d'Hendecourt, L. L.; Meierhenrich, U. J. Ribose and related sugars from ultraviolet irradiation of interstellar ice analogs. *Science* **2016**, *352*, 208.
- (19) de Marcellus, P.; Meinert, C.; Myrgorodska, I.; Nahon, L.; Buhse, T.; d'Hendecourt, L. L. S.; Meierhenrich, U. J. Aldehydes and sugars from evolved precometary ice analogs: Importance of ices in astrochemical and prebiotic evolution. *Proc. Natl. Acad. Sci. U. S. A.* **2015**, *112*, 965.
- (20) Engel, M. H.; Macko, S. A. Isotopic evidence for extraterrestrial non-racemic amino acids in the Murchison meteorite. *Nature* **1997**, *389*, 265.
- (21) Altwegg, K.; Balsiger, H.; Bar-Nun, A.; Berthelier, J.-J.; Bieler, A.; Bochler, P.; Briois, C.; Calmonte, U.; Combi, M. R.; Cottin, H.; De Keyser, J.; Dhooche, F.; Fiethe, B.; Fuselier, S. A.; Gasc, S.; Gombosi, T. I.; Hansen, K. C.; Haessig, M.; Jäckel, A.; Kopp, E.; Korth, A.; Le Roy, L.; Mall, U.; Marty, B.; Mousis, O.; Owen, T.; Rème, H.; Rubin, M.; Sémon, T.; Zou, C.-Y.; Hunter Waite, J.; Wurz, P. Prebiotic chemicals—amino acid and phosphorus—in the coma of comet 67P/Churyumov-Gerasimenko. *Science Advances* **2016**, *2*, e1600285.
- (22) Muñoz Caro, G. M.; Meierhenrich, U. J.; Schutte, W. A.; Barbier, B.; Arcones Segovia, A.; Rosenbauer, H.; Thiemann, W. H. P.; Brack, A.; Greenberg, J. M. Amino acids from ultraviolet irradiation of interstellar ice analogues. *Nature* **2002**, *416*, 403.
- (23) Mardiyukov, A.; Eckhardt, A. K.; Schreiner, P. R. 1,1-Ethenediol: The Long Elusive Enol of Acetic Acid. *Angew. Chem., Int. Ed.* **2020**, *59*, 5577.
- (24) Mardiyukov, A.; Keul, F.; Schreiner, P. R. 1,1,2-Ethenetriol: The Enol of Glycolic Acid, a High-Energy Prebiotic Molecule. *Angew. Chem., Int. Ed.* **2021**, *60*, 15313.
- (25) Mardiyukov, A.; Keul, F.; Schreiner, P. R. Preparation and characterization of the enol of acetamide: 1-aminoethanol, a high-energy prebiotic molecule. *Chemical Science* **2020**, *11*, 12358.
- (26) Ruttink, P. J. A.; Dekker, L. J. M.; Luider, T. M.; Burgers, P. C. Complexation of divalent metal ions with diols in the presence of anion auxiliary ligands: zinc-induced oxidation of ethylene glycol to glycolaldehyde by consecutive hydride ion and proton shifts. *J. Mass Spectrom.* **2012**, *47*, 869.
- (27) Lasne, M.-C.; Ripoll, J.-L. Reactions retrodieniques XIII - thermolyse éclair des (Z) et (E) dihydroxy-11, 12 ethano-9,10 dihydro-9,10 anthracenes: synthèse des (Z) et (E) ethenediols-1,2. *Tetrahedron Lett.* **1982**, *23*, 1587.
- (28) Abplanalp, M. J.; Gozem, S.; Krylov, A. I.; Shingledecker, C. N.; Herbst, E.; Kaiser, R. I. A study of interstellar aldehydes and enols as tracers of a cosmic ray-driven nonequilibrium synthesis of complex organic molecules. *Proc. Natl. Acad. Sci. U. S. A.* **2016**, *113*, 7727.
- (29) Bennett, C. J.; Jamieson, C. S.; Osamura, Y.; Kaiser, R. I. A combined experimental and computational investigation on the synthesis of acetaldehyde [$\text{CH}_3\text{CHO}(\text{X}^1\text{A}')$] in interstellar ices. *Astrophys. J.* **2005**, *624*, 1097.
- (30) Maity, S.; Kaiser, R. I.; Jones, B. M. Infrared and reflectron time-of-flight mass spectroscopic study on the synthesis of glycolaldehyde in methanol (CH_3OH) and methanol-carbon monoxide ($\text{CH}_3\text{OH}-\text{CO}$) ices exposed to ionization radiation. *Faraday Discuss.* **2014**, *168*, 485.
- (31) Öberg, K. I.; Boogert, A. C. A.; Pontoppidan, K. M.; van den Broek, S.; van Dishoeck, E. F.; Bottinelli, S.; Blake, G. A.; Evans, N. J. The Spitzer Ice Legacy: ice evolution from cores to protostars. *Astrophys. J.* **2011**, *740*, 109.
- (32) Gibb, E. L.; Whittet, D. C. B.; Boogert, A. C. A.; Tielens, A. G. G. M. Interstellar ice: the Infrared Space Observatory Legacy. *Astrophys. J., Suppl. Ser.* **2004**, *151*, 35.
- (33) Turner, B. E.; Apponi, A. J. Microwave detection of interstellar vinyl alcohol, $\text{CH}_2=\text{CHOH}$. *Astrophys. J.* **2001**, *561*, L207.
- (34) Halfen, D. T.; Apponi, A. J.; Woolf, N.; Polt, R.; Ziurys, L. M. A systematic study of glycolaldehyde in Sagittarius B2(N) at 2 and 3 mm: Criteria for detecting large interstellar molecules. *Astrophys. J.* **2006**, *639*, 237.
- (35) Hollis, J. M.; Lovas, F. J.; Jewell, P. R. Interstellar glycolaldehyde: the first sugar. *Astrophys. J.* **2000**, *540*, L107.
- (36) Drouin, D.; Couture, A. R.; Joly, D.; Tastet, X.; Aimez, V.; Gauvin, R. CASINO V2.42—A fast and easy-to-use modeling tool for scanning electron microscopy and microanalysis users. *Scanning* **2007**, *29*, 92.
- (37) Hilbig, R.; Wallenstein, R. Tunable VUV radiation generated by two-photon resonant frequency mixing in xenon. *IEEE J. Quantum Electron.* **1983**, *19*, 194.
- (38) Ehrenfreund, P.; Boogert, A. C. A.; Gerakines, P. A.; Tielens, A. G. M.; van Dishoeck, E. F. Infrared spectroscopy of interstellar apolar ice analogs. *Astron. Astrophys.* **1997**, *328*, 649.
- (39) Frisch, M. J.; Trucks, G. W.; Schlegel, H. B.; Scuseria, G. E.; Robb, M. A.; Cheeseman, J. R.; Scalmani, G.; Barone, V.; Petersson, G. A.; Nakatsuji, H.; Li, X.; Caricato, M.; Marenich, A. V.; Bloino, J.; Janesko, B. G.; Gomperts, R.; Mennucci, B.; Hratchian, H. P.; Ortiz, J. V.; Izmaylov, A. F.; Sonnenberg, J. L.; Williams-Young, D.; Ding, F.; Lipparini, F.; Egidi, F.; Goings, J.; Peng, B.; Petrone, A.; Henderson, T.; Ranasinghe, D.; Zakrzewski, V. G.; Gao, J.; Rega, N.; Zheng, G.; Liang, W.; Hada, M.; Ehara, M.; Toyota, K.; Fukuda, R.; Hasegawa, J.; Ishida, M.; Nakajima, T.; Honda, Y.; Kitao, O.; Nakai, H.; Vreven, T.; Throssell, K.; Montgomery, J. A., Jr.; Peralta, J. E.; Ogliaro, F.; Bearpark, M. J.; Heyd, J. J.; Brothers, E. N.; Kudin, K. N.; Staroverov, V. N.; Keith, T. A.; Kobayashi, R.; Normand, J.; Raghavachari, K.; Rendell, A. P.; Burant, J. C.; Iyengar, S. S.; Tomasi, J.; Cossi, M.; Millam, J. M.; Klene, M.; Adamo, C.; Cammi, R.; Ochterski, J. W.; Martin, R. L.; Morokuma, K.; Farkas, O.; Foresman, J. B.; Fox, D. J. *Gaussian 16, Revision A.03*; Gaussian Inc., Wallingford, CT, 2016.
- (40) Becke, A. D. Density-functional exchange-energy: Approximation with correct asymptotic behavior. *Phys. Rev. A: At., Mol., Opt. Phys.* **1988**, *38*, 3098.
- (41) Lee, C.; Yang, W.; Parr, R. G. Development of the Colle-Salvetti correlation-energy formula into a functional of the electron density. *Phys. Rev. B: Condens. Matter Mater. Phys.* **1988**, *37*, 785.
- (42) Becke, A. D. Density-functional thermochemistry. III. The role of exact exchange. *J. Chem. Phys.* **1993**, *98*, 5648.
- (43) Dunning, J.; Thom, H. Gaussian basis sets for use in correlated molecular calculations. I. The atoms boron through neon and hydrogen. *J. Chem. Phys.* **1989**, *90*, 1007.
- (44) Bartlett, R. J.; Watts, J. D.; Kucharski, S. A.; Noga, J. Non-iterative fifth-order triple and quadruple excitation energy corrections in correlated methods. *Chem. Phys. Lett.* **1990**, *165*, 513.
- (45) Čížek, J. On the correlation problem in atomic and molecular systems. Calculation of wavefunction components in Ursell-type expansion using quantum-field theoretical methods. *J. Chem. Phys.* **1966**, *45*, 4256.
- (46) Raghavachari, K. Electron correlation techniques in quantum chemistry: Recent advances. *Annu. Rev. Phys. Chem.* **1991**, *42*, 615.
- (47) Stanton, J. F. Why CCSD(T) works: a different perspective. *Chem. Phys. Lett.* **1997**, *281*, 130.

- (48) Peterson, K. A.; Woon, D. E.; Dunning, T. H. Benchmark calculations with correlated molecular wave functions. IV. The classical barrier height of the $\text{H} + \text{H}_2 \rightarrow \text{H}_2 + \text{H}$ reaction. *J. Chem. Phys.* **1994**, *100*, 7410.
- (49) Harvey, K. B.; Ogilvie, J. F. Infrared absorption of formaldehyde at low temperatures: evidence for multiple trapping sites in an argon matrix. *Can. J. Chem.* **1962**, *40*, 85.
- (50) Bennett, C. J.; Kaiser, R. I. On the formation of glycolaldehyde (HCOCH_2OH) and methyl formate (HCOOCH_3) in interstellar ice analogs. *Astrophys. J.* **2007**, *661*, 899.
- (51) Saenko, E. V.; Feldman, V. I. Radiation-induced transformations of methanol molecules in low-temperature solids: a matrix isolation study. *Phys. Chem. Chem. Phys.* **2016**, *18*, 32503.
- (52) Ryazantsev, S. V.; Tyurin, D. A.; Feldman, V. I. Experimental determination of the absolute infrared absorption intensities of formyl radical HCO. *Spectrochim. Acta, Part A* **2017**, *187*, 39.
- (53) Bennett, C. J.; Chen, S.-H.; Sun, B.-J.; Chang, A. H. H.; Kaiser, R. I. Mechanical Studies on the Irradiation of Methanol in Extraterrestrial Ices. *Astrophys. J.* **2007**, *660*, 1588.
- (54) Kostko, O.; Bandyopadhyay, B.; Ahmed, M. Vacuum ultraviolet photoionization of complex chemical systems. *Annu. Rev. Phys. Chem.* **2016**, *67*, 19.
- (55) Bergantini, A.; Abplanalp, M. J.; Pokhilko, P.; Krylov, A. I.; Shingledecker, C. N.; Herbst, E.; Kaiser, R. I. A combined experimental and theoretical study on the formation of interstellar propylene oxide ($\text{CH}_3\text{CHCH}_2\text{O}$)—a chiral molecule. *Astrophys. J.* **2018**, *860*, 108.
- (56) Maity, S.; Kaiser, R. I.; Jones, B. M. Formation of complex organic molecules in methanol and methanol–carbon monoxide ices exposed to ionizing radiation – a combined FTIR and reflectron time-of-flight mass spectrometry study. *Phys. Chem. Chem. Phys.* **2015**, *17*, 3081.
- (57) Bell, F.; Ruan, Q. N.; Golan, A.; Horn, P. R.; Ahmed, M.; Leone, S. R.; Head-Gordon, M. Dissociative photoionization of glycerol and its dimer occurs predominantly via a ternary hydrogen-bridged ion–molecule complex. *J. Am. Chem. Soc.* **2013**, *135*, 14229.
- (58) Abplanalp, M. J.; Góbi, S.; Kaiser, R. I. On the formation and the isomer specific detection of methylacetylene (CH_3CCH), propene (CH_3CHCH_2), cyclopropane ($c\text{-C}_3\text{H}_6$), vinylacetylene (CH_2CHCCH), and 1,3-butadiene ($\text{CH}_2\text{CHCHCH}_2$) from interstellar methane ice analogues. *Phys. Chem. Chem. Phys.* **2019**, *21*, 5378.
- (59) Kiselev, V. G.; Swinnen, S.; Nguyen, V. S.; Gritsan, N. P.; Nguyen, M. T. Fast reactions of hydroxycarbenes: tunneling effect versus bimolecular processes. *J. Phys. Chem. A* **2010**, *114*, 5573.
- (60) Schreiner, P. R. Tunneling control of chemical reactions: the third reactivity paradigm. *J. Am. Chem. Soc.* **2017**, *139*, 15276.
- (61) Simons, M. A. J.; Lamberts, T.; Cuppen, H. M., Formation of COMs through CO hydrogenation on interstellar grains. *Astron. Astrophys.* **2020**, *634*, A52
- (62) So, S.; Wille, U.; da Silva, G. A Theoretical Study of the Photoisomerization of Glycolaldehyde and Subsequent OH Radical-Initiated Oxidation of 1,2-Ethenediol. *J. Phys. Chem. A* **2015**, *119*, 9812.
- (63) Schreiner, P. R.; Reisenauer, H. P.; Ley, D.; Gerbig, D.; Wu, C.-H.; Allen, W. D. Methylhydroxycarbene: Tunneling Control of a Chemical Reaction. *Science* **2011**, *332*, 1300.
- (64) Kleimeier, N. F.; Kaiser, R. I. Interstellar Enolization-Acetaldehyde (CH_3CHO) and Vinyl Alcohol ($\text{H}_2\text{CCH}(\text{OH})$) as a Case Study. *ChemPhysChem* **2021**, *22*, 1229.
- (65) Chuang, K. J.; Fedoseev, G.; Ioppolo, S.; van Dishoeck, E. F.; Linnartz, H. H-atom addition and abstraction reactions in mixed CO, H_2CO and CH_3OH ices - an extended view on complex organic molecule formation. *Mon. Not. R. Astron. Soc.* **2016**, *455*, 1702.
- (66) Fedoseev, G.; Cuppen, H. M.; Ioppolo, S.; Lamberts, T.; Linnartz, H. Experimental evidence for glycolaldehyde and ethylene glycol formation by surface hydrogenation of CO molecules under dense molecular cloud conditions. *Mon. Not. R. Astron. Soc.* **2015**, *448*, 1288.
- (67) Chen, L.; Woon, D. E. A theoretical investigation of the plausibility of reactions between ammonia and carbonyl species (formaldehyde, acetaldehyde, and acetone) in interstellar ice analogs at ultracold temperatures. *J. Phys. Chem. A* **2011**, *115*, 5166.
- (68) Kua, J.; Avila, J. E.; Lee, C. G.; Smith, W. D. Mapping the kinetic and thermodynamic landscape of formaldehyde oligomerization under neutral conditions. *J. Phys. Chem. A* **2013**, *117*, 12658.
- (69) Pizzarello, S.; Schrader, D. L.; Monroe, A. A.; Lauretta, D. S. Large enantiomeric excesses in primitive meteorites and the diverse effects of water in cosmochemical evolution. *Proc. Natl. Acad. Sci. U. S. A.* **2012**, *109*, 11949.